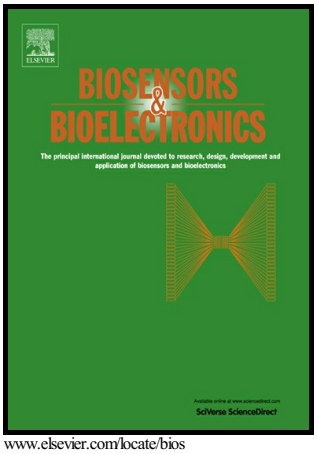

www.elsevier.com/locate/bios

Copper (II)-ploy-L-histidine functionalized multi walled carbon nanotubes as efficient mimetic enzyme for sensitive electrochemical detection of salvianic acid A

Zihua Wang, Yuan Chen, Wenhao Dong, Jiexin Zhou, Bingkai Han, Jun Jiao, Lintao Lan, Peng Miao, Qiang Chen

PII: S0956-5663(18)30688-2
DOI: https://doi.org/10.1016/j.bios.2018.09.007
Reference: BIOS10747

To appear in: *Biosensors and Bioelectronic*

Received date: 12 June 2018
Revised date: 31 August 2018
Accepted date: 1 September 2018

Cite this article as: Zihua Wang, Yuan Chen, Wenhao Dong, Jiexin Zhou, Bingkai Han, Jun Jiao, Lintao Lan, Peng Miao and Qiang Chen, Copper (II)-ploy-L-histidine functionalized multi walled carbon nanotubes as efficient mimetic enzyme for sensitive electrochemical detection of salvianic acid A, *Biosensors and Bioelectronic,* https://doi.org/10.1016/j.bios.2018.09.007

Copper (II)-ploy-L-histidine functionalized multi walled carbon nanotubes as efficient mimetic enzyme for sensitive electrochemical detection of salvianic acid A

Zihua Wang[a], Yuan Chen[a], Wenhao Dong[a], Jiexin Zhou[a], Bingkai Han[a], Jun Jiao[a], Lintao Lan[a], Peng Miao[b,*], Qiang Chen[a,*]

[a]*The Key Laboratory of Bioactive Materials Ministry of Education, College of Life Science, Nankai University, Weijin Road No.94, Tianjin, 300071, PR China*

[b]*Suzhou Institute of Biomedical Engineering and Technology, Chinese Academy of Sciences, Suzhou, 215163, PR China*

[*]Corresponding author A: Dr. Q. Chen, Tel.: +86 022 23506122, Email: qiangchen@nankai.edu.cn.

*Corresponding author B: Dr. P. Miao, Tel.: +86 512 69588279, Email: miaopeng@sibet.ac.cn.

Abstract

In this work, carboxylated multi walled carbon nanotubes (CMWCNTs) were firstly prepared and functionalized with poly-L-histidine (PLH), which were then chelated with copper (II) ions to from the nanocomposites of Cu(II)-PLH-CMWCNTs. The nanocomposites could be exploited as an efficient mimic enzyme for sensitive

electrochemical detection of salvianic acid A (SAA). Cu(II)-PLH-CMWCNTs owned good charge transfer property and excellent synergetic catalytic effect between the overoxidized imidazole groups and the copper redox-active units. Therefore, highly sensitive electrochemical response to SAA was achieved under optimum experimental conditions. A good linear relationship between differential pulse voltammetry (DPV) peak current and the SAA concentration was established in the range of 0.4 to 1000 μM. A low detection limit of 0.037 μM and a sensitivity of 0.27 μA μM^{-1} cm^{-2} were achieved. The developed biosensor also had advantages of good repeatability, stability and high selectivity, thus, it was successfully applied to the determination of SAA in real samples with satisfactory results, which may have great potential for further exploitation of electroanalysis applications.

Keywords: Cu(II); Poly-L-histidine; Multi walled carbon nanotubes; Mimetic enzyme; Salvianic acid A; Differential pulse voltammetry.

1. Introduction

Since the discovery and successful application of artemisinin in the treatment of malaria (Youyou 2016), natural drug molecules from medical plants have attracted tremendous interests. Salvianic acid A (SAA), also termed as D-(+)-β-3,4-ihydroxyphenyl-lactic acid, is isolated from *Salvia miltiorrhiza* (Fam. Labiatae), which has many excellent bioactivities. For example, it protects myocardial mitochondrial membranes from ischemia-reperfusion (Zhao et al. 1996) and prevents cytotoxicity causedcell damage (Wang and Xu 2005) . Oxidative stress, carbon tetrachloride induced acute liver injury (Wang et al. 2007; Zhi-ming et al. 2007) , and

lipid peroxidation can also be inhibited by SAA (Wang et al. 2005) . Therefore, it's of great importance to investigate the function mechanism of SAA and develop low-cost, simple, efficient and sensitive method for the detection of SAA. So far, some approaches, including spectroscopic method (Liu et al. 2011) , chromatographic method (Chen-Long and Guang-Rong 2015; Zhao et al.), high performance liquid chromatography–mass spectrometry (Lixia et al. 2008) and electrochemical method (Zhao et al. 2013) , have been developed for SAA determination. Among them, electrochemical method attracts more and more attention due to the advantages of cost-effectiveness, simple operation, fast response, and high sensitivity. Moreover, electrochemical method also helps analysis the redox reactions of the drug substances and provide important pharmacological and pharmacokinetic information. However, up to now, there are only few papers reported concerning SAA analysis based on electrochemical techniques(Zhao et al. 2013). More advanced electrochemical methods for SAA assay should be developed.

Enzymes are the most abundant, efficient and specific catalysts in nature. However, their poor stabilities originated from the intrinsic nature seriously limit the biosensing applications (Weckhuysen Bert et al. 1996) .To overcome these disadvantages, non-enzymatic biosensors utilizing mimetic enzymes have been proposed. The building of the active center (or an analogy) is the core part in enzyme mimicking, in which transition metal ion complexes are commonly used. Copper (Cu) ion have been widely considered as a catalyst in the oxidation reactions of various organic substrates by molecular oxygen. It has been found that the complexation of Cu(II) by certain

ligands like poly-L-histidine (PLH), o-phenanthroline, dipyridyl and azide modifies its catalytic activity (Pecht et al. 1967a) . In certain oxidations , Cu(II)-PLH complex a much higher catalytic activity than Cu(II) in the aquo or acetato complexes (Levitzki et al. 1965) . Pecht et al. studied the copper-catalyzed oxidation by molecular oxygen of ascorbate, homogentisate ions etc., and found that the kinetic characteristic of the Cu(II)-PLH catalyzed oxidation reactions expressed similarity with some enzymatic oxidation processes(Pecht et al. 1967a) . Ueda et al. studied the autoxidation of L-ascorbate catalyzed by Cu(II)-PLH, concluded that the reaction obeyed the Michaelis-Menten kinetic, and found that the labile copper ions concentrated in the PLH phase might be the catalytically species (Jun-ichi and Akira 1984) . Therefore, the combination of Cu(II) with PLH may have great potential utility in the field of electroanalytical chemistry.

Herein, we report an enzyme-mimicking electrochemical biosensor based on the Cu(II)-PLH functionalized carboxylated multi walled carbon nanotubes (CMWCNTs) for high-sensitivity detection of SAA. Due to the π–π stacking interaction between the imidazole groups of PLH chain and CMWCNTs, electron mobility is effectively increased since electrons can delocalize over all the conjugated composites. In addition, CMWCNTs can largely enhance the electrode active surface area, which is very beneficial to the redox reaction of SAA. Moreover, the excellent synergetic catalytic effect between the overoxidized imidazole groups and the copper redox-active units results in a high catalytic activity to SAA oxidation. On the basis of these extraordinary properties, a simple and efficient method is successfully

established for the electrochemical detection of SAA.

2. Experimental Section

2.1 Chemicals and reagents

PLH, (MW 5,000-25,000), N-(3-dimethylaminopropyl)-N′-ethylcarbodiimide hydrochloride (EDC) and N-hydroxysuccinimide (NHS) were purchased from Sigma–Aldrich (USA). MWCNTs (30~50 nm diameter, 10 μm average length and 95% purity) were purchased from Institute of Organic Chemistry, Chinese Academy of Sciences (Chengdu, China). SAA, 3,4-dihydroxy benzaldehyde (protocatechuic aldehyde, PA), 1,2-benzenediol (catechol, CC), ascorbic acid (AA), uric acid (UA) and glucose were purchased from Aladdin Industrial Corporation (Shanghai, China). Cupric chloride ($CuCl_2$), sodium dihydrogen phosphate ($NaH_2PO_4 \cdot 2H_2O$), dibasic sodium phosphate ($Na_2HPO_4 \cdot 12H_2O$), potassium chloride (KCl), potassium ferricyanide ($K_3Fe[(CN)_6]$), sulfuric acid (H_2SO_4, 98%), nitric acid (HNO_3, 65%) were purchased from Tianjin Damao Chemical Reagent Factory (Tianjin, China). All other reagents were of analytical reagent grade and used as received without any further purification. All the aqueous solutions were prepared by deionized water.

2.2 Preparation of the Cu(II)-PLH-CMWCNTs

CMWCNTs were prepared by the mixed acid treatment according to our previously reported work with a small modification. 20 mg raw MWCNTs were treated with 20 mL mixture of sulfuric acid and nitric acid (3:1, v/v) at 55 °C for 6 h under ultrasonic processing (Ma et al. 2015) . Afterward, the product was centrifuged and washed with

deionized water for several times until nearly neutral pH condition. The precipitation was vacuum dried at 80 °C, and then CMWCNTs were obtained.

Platinum electrode (PtE) was polished with 0.3, 0.1, 0.05 μm alumina powders sequentially, immersed in a mixture of sulfuric acid and hydrogen peroxide (3:1, v/v) at 90 °C for 10 min and ultrasonically cleaned alternately in deionized water and absolute ethanol for 2 min 3 times, which was finally dried with high-purity nitrogen.

2 mM EDC and 5 mM NHS were added to 1 mg/mL CMWCNTs, which were dispersed in 0.1 M phosphate buffer solution (PBS, pH 6.0), and reacted for 15 min at room temperature, followed by adding 20 mM 2-mercaptoethanol to quench the EDC/NHS. CMWCNTs were separated from the excess agents by centrifugation and were then redissolved in PBS (pH 7.0). The functionalization of PLH was performed by adding 1 mg/mL PLH (dissolved in 0.1 M HCl) to react for 2 h. The Cu(II) complexation was synthesized by adding 0.1 M $CuCl_2$ to react for another 2h. Then, the Cu(II) -PLH-CMWCNTs composites were obtained by centrifugation and resuspension, and quantified to equivalent 1 mg/mL CMWCNTs. Subsequently, a SAA sensor was developed by droplet-coating 10 μL of the above composites onto the surface of a freshly cleaned PtE, and denoted as Cu(II)-PLH-CMWCNTs/PtE, which was dried and stored at room temperature before use. The fabrication procedure is shown in Scheme S1.

2.3 Electrochemial measurements

A potentiostat-galvanostat electrochemical workstation (EG&GPARC, Model 283 with M270 software) was applied for all the electrochemical experiments, with a

typical three-electrode system of an Ag/AgCl (saturated with KCl) as the reference electrode, a platinum wire (φ=1 mm) as the counter electrode and a modified PtE(φ=3 mm) as the working electrode. Transmission electron microscope (FEI, Tecnai G2 F20) was applied for characterizing the prepared materials. Fourier transform infrared spectroscopies (FTIR) were collected on Bruker TENSOR37 (German). Raman spectra were collected on Bruker RFS 100/S (German). X-ray proton emission (XPS) were collected on Escalab 250Xi (America). All measurements were performed at room temperature, approximately 25 °C.

3. Results and discussion

3.1 Characterizations of the Cu(II)-PLH-CMWCNTs composites

FTIR spectroscopy is a powerful tool in characterizing the structure and components of the materials. Fig.S1 displayed the FTIR spectra of MWCNTs (curve a), CMWCNTs (b), PLH-CMWCNTs (c) and Cu(II)-PLH-CMWCNTs (d). Comparing curve c to curve a and b, the increased stretching frequencies of C═C around 1623 cm^{-1}, C═N around 1608 cm^{-1}, and C─N around 1536 cm^{-1}, were attributed to the imidazole groups of PLH, and the OH stretching around 1000 cm^{-1} was attributed to the free carboxylic acid of PLH. The result indicated that PLH had successfully immobilized on the CMWCNTs (J. et al. 2007; Saleh and Gupta 2011; Vilian and Chen 2014). As for curve d, the decrease of the above stretching frequencies in curve d suggested the chelation of Cu(II). The Raman analysis of the Cu(II)-PLH-CMWCNTs nanocomposites was presented in the supplementary

material.

Microstructures of the carbon nanotubes composites were characterized by Transmission Electron Microscope (TEM) and Energy-dispersive X-ray spectroscopy (EDX). Fig. 1A showed the hollow tubular structures of raw MWCNTs. Mixed acid treated CMWCNTs with defects and open ends could been seen clearly in Fig. 1B. Fig. 1C showed the PLH functionalized CMWCNTs with a thin layer of PLH. As shown in Fig. 1D, EDX spectrum indicated that the elementary composition of the nanocomposites. The N peak was arose from the modification of PLH, the presence of Cu element (5.4 wt%) was attributed to the chelation of Cu(II), while the Mo peaks were resulted from the molybdenum substrate. In summary, the Cu(II)-PLH-CMWCNTs composites were prepared successfully.

X-ray photoelectron spectroscopy (XPS) was applied to further ascertain the surface component of the nanocomposites. Fig. 1E showed the XPS spectrum of the Cu(II)-PLH-CMWCNTs, which exhibited the binding energies of C1s, O1s, N1s and Cu2p. Fig. 1F,G,H presented the individual high-resolution XPS spectra of elements C, N and Cu. In Fig. 1F, C1s at 284.4, 286.8 and 288.3 eV for samples could be due to C─C, C─O and C═O bonds respectively, while the new peak observed at 285.8 eV was resulted from the C─N of PLH-CMWCNTs. In Fig. S3, compared to the CMWCNTs and PLH-CMWCNTs, the emerging peak at 400.0 eV (N1s) was attributed to the insertion of imidazole groups on the PLH side chain. In Fig. 1G, the high-resolution XPS spectrum of N 1s shows peaks centred at 398.6, 399.9 and 401.3 eV corresponding to ─C═N─C─, ─C─N─H and $-N^{+}-$, respectively. The results

indicated that the PLH have successfully modified on CMWCNTs. As shown in Fig. 1H, The characteristic peaks were observed at 932.3 and 954.6 eV, which was the typical character of Cu $2p_{3/2}$ and $Cu2p_{1/2}$. The satellite peaks range from 940 to 945 eV indicated that the chelation of Cu element existed in the form of Cu(II).

3.2 Electrochemical performance of the Cu(II)-PLH-CMWCNTs/PtE

Cyclic voltammogram (CV) in ferricyanide system is a generally accepted method to evaluate the electroactive surface area and the charge transfer properties of the fabricated electrodes (Fang et al. 2015) . The cyclic voltammograms of the bare PtE, CMWCNTs, PLH-CMWCNTs, and Cu(II)-PLH-CMWCNTs modified PtE conducted in 10 mM $K_3[Fe(CN)_6]$ solution with 0.1 M KCl were shown in Fig. 2A. All the above electrodes presented a couple of well-defined redox peaks of $Fe^{2+/3+}$ at 180/260 mV. For the Cu(II)-PLH-CMWCNTs/PtE, there was another couple well-defined redox peaks of $Cu^{2+/3+}$ at 680/750 mV, which attributed to the chelation of Cu(II). The effective surface areas of the electrodes could be calculated from the Randles–Sevcik equation (1)(Ramanathan et al. 2016).

$$i_p = 2.69 \times 10^5 n^{3/2} \mathrm{D}^{1/5} \mathrm{C}_0 v^{1/2} A_{eff} \quad (1)$$

where i_p was the redox peak current (□A), n represented the number of electrons transferred in the redox reaction, D was related to the diffusion coefficient of the molecule in solution which was $(6.70 \pm 0.02) \times 10^{-6}$ cm^2 s^{-1}, C_0 was the concentration of the probe molecule which was 10 mM, v was the scan rate (50 mV s^{-1}), and A_{eff} corresponded to the effective surface area of the electrode (cm^2). The effective surface

area of the Cu(II)-PLH-CMWCNTs/PtE was calculated be 0.17 cm^2, which was 1.12, 2.02 and 2.44 times higher than those of the PLH-CMWCNTs/PtE, CMWCNTs/PtE and bare PtE. The effective surface area of PLH-CMWCNTs/PtE was 1.80 times higher than CMWCNTs/PtE, which was significantly higher than the ratio of CMWCNTs/PtE to bare PtE (viz. 1.21). Suggested that the functionalization of PLH could remarkably improve the charge transfer property of CMWCNTs, which finally achieved the high sensitivity of the fabricated biosensor.

Electrocatalytic performance of the Cu(II)-PLH-CMWCNTs/PtE toward SAA was investigated in Fig. 2B and 2C. Fig. 2B displayed the electrochemical behaviors of SAA in PBS (pH 3.0) at the bare PtE (curve a), CMWCNTs/PtE (b), PLH-CMWCNTs/PtE (c) and Cu(II)-PLH-CMWCNTs/PtE (d), respectively. For the bare PtE, the oxidation peak current of SAA was 44.2 μA and the oxidation peak potential was 630 mV. By comparison, the peak current of the CMWCNTs/PtE increased to 77.3 μA and oxidation peak potential was 310 mV smaller. This could be attributed to the high electronic conductivity and large effective surface area of the CMWCNTs. For the PLH-CMWCNTs/PtE, the peak current increased to 110.6 μA and the peak separation further decreased 40 mV. This mainly attributed to the aromatic π–π stacking interaction between PLH and CMWCNTs, which enhanced the high charge transfer properties and enlarged effective surface areas. For the Cu(II)-PLH-CMWCNTs/PtE, the peak current increased to 134.9 μA, which could be attributed to the excellent synergetic catalytic effect between the unique structure with PLH and the copper redox-active units towards the oxidation of SAA. To visually

compared catalytic ability of different modified electrodes, Fig S4 exhibited the bare PtE (Fig S4A), CMWCNTs/PtE (B), PLH-CMWCNTs/PtE (C) and Cu(II)-PLH-CMWCNTs/PtE (D) electrochemical response in the absence and presence of SAA. Among them, Cu(II)-PLH-CMWCNTs/PtE have a relatively biggest oxidation current in 0.6 mM SAA, which was due to larger electroactive surface area, higher charge transfer properties and superior electrocatalytic performance for SAA. In Fig. 2C, the Cu(II)-PLH-CMWCNTs/PtE showed excellent electrocatalytic activity towards different levels of SAA. Compare with curve (a), we can clearly observed a pair of redox peaks around -80 mV and 300 mV in curve (b), in curve (c) and in curve (d), the response current increased with increasing of SAA concentration, which was attributed to Cu(II)/Cu(I) redox-active units mediate SAA electrocatalytic oxidation. Along with the increase of SAA concentration, the redox current of Cu(II)/Cu(I) at 0/-150 mV increased slightly, indicated that the amount of Cu(II) involved in the electrocatalytic reaction was positively correlated with the SAA concentration within certain limitation.

This highly efficient electrocatalytic performance suggested that the Cu(II)-PLH-CMWCNTs composites based on the particular structure with highly delocalized and conjugated π system of PLH and the copper redox-active units had excellent electrocatalytic ability towards the oxidation of SAA. This phenomenon could be summarized as the synergetic effect: (1) CMWCNTs could enlarge electrode active surface area, which was helpful to the redox reaction process between SAA and

copper redox-active units(Yan et al. 2016); (2) PLH changed the morphology of CMWCNTs via amide bonds and π–π stacking interaction, which was very important to optimize the electrochemical performance of CMWCNTs and enhance the electrons transport; (3) imidazole groups of PLH can be overoxidized at high anodic potentials, during the overoxidized process oxygen-containing groups such as carbonyl and carboxyl were introduced to imidazole units, which was beneficial to improve the permselective and anti-interference properties of the biosensor; (4) there is a synergetic catalytic effect between the overoxidized imidazole groups and copper redox-active units (Liu et al. 2014). The proposed mechanism of Cu(II)/Cu(I) redox-active units mediate SAA electrocatalytic oxidation was illustrated in Scheme. 1 (Jiang et al. 2015; Pecht et al. 1967b). Therefore, Cu(II)-PLH-CMWCNTs/PtE can be a good choice for the electrochemical detection of SAA.

3.3 Effect of buffer pH

The pH effect on the electrochemical response of SAA on Cu(II)-PLH-CMWCNTs/PtE was investigated in the pH range from 3.0 to 8.0 with the results shown in Fig. S5. With the increasing of pH, the redox peak potentials of SAA shifted to the negative direction (Fig. S5A), which indicated that protons involved in the electrochemical reaction. In the selected pH range, the linear relationship between the formal peak potential ($E^{0'}$) and pH was established with the equation as $E^{0'}$ (mV)=60.17pH-619.59 (R^2=0.998) (as shown in Fig. S5B). The slope

value of 60.17 mV/pH is quite close to the Nernstian value of 59 mV/pH at 25 °C, indicated an equal number of protons and electrons involved in the electrochemical reaction (Wang et al. 2014; Yan et al. 2016). The relationship between oxidation peak current and buffer pH was showed in the inset of Fig. S5B. The maximum value appeared at pH 3.0, which was chosen as the optimal pH for the detection of SAA. At the same time, lower pH had also been investigated, however the current response was not stable (dates were not given), which might be caused by the stability of chelate copper ions decreasing at lower pH.

3.4 Effect of scan rate

The effect of scan rate at the Cu(II)-PLH-CMWCNTs/PtE was investigated by a typical cyclic voltammetry (as shown in Fig. S6A). It could be seen that both the oxidation and reduction currents of SAA increased linearly with the square root of the scan rate in the range from 10.0 to 100.0 mV s^{-1}. As shown in Fig. S6B, the redox peak current (I_p) exhibited a good linear relationship with the square root of scan rate ($v^{1/2}$). Tow linear regression equations were expressed as I_{pc}(μA) =16.5730$v^{1/2}$-18.5025 (v in mV s^{-1}, R^2=0.998) and I_{pa}(μA) =-13.3366$v^{1/2}$+19.7275 (v in mV s^{-1}, R^2=0.999), indicated a diffusion-controlled electrochemical process. The diffusion coefficient of SAA was calculated according to the equation (2) (Yan et al. 2016):

$$I_p = 2.69 \times 10^5 (\text{A s mol}^{-1} v^{-1/2}) A n^{3/2} {D_0}^{1/2} C_0 v^{1/2} \quad (2)$$

Where I_p was the redox peak current, A was the effective electrochemical electrode area, n was the number of electron involved in the rate determining step,

D_0 was the diffusion coefficient, C_0 was the bulk concentration of SAA, and $v^{1/2}$ was the square root of scan rate. By calculating the slope and putting the necessary values to the equation, D_0 value was calculated as 6.57×10^{-6} cm^2 s^{-1}.

3.5 Electrochemical determination of SAA

Differential pulse voltammetry (DPV) was used for the quantitative determination of SAA in PBS pH 3.0 with various concentrations of SAA. Fig. 3A showed the DPV determination of SAA with concentrations ranging from 0.1 μM to 3500 μM (inset shows the lower concentrations from 0.1 μM to 3.0 μM). The electrocatalytic oxidation currents of SAA increased gradually with increasing of the concentrations. A calibration curve was fitted and shown in Fig. 3B after five independent tests (inset showed the linearity from 0.4 to 3.0 μM). The response currents exhibited a linear variation with the increasing concentrations of SAA over the range of 0.4 μM to 1000 μM. The linear regression equation was expressed as y=0.01884x+3.98898 (R^2 =0.99947). The limit of detection (LOD) was calculated to be 0.037 μM at the signal-to-noise of 3 (S/N=3). Moreover, the sensitivity of the fabricated biosensor was calculated from the slope of the curve and found to be 0.27 μA μM^{-1} cm^{-2}. For further comparison, the different mothods of SAA detection were summarized in Table S1. Among them, electrochemical method could be recommended for the SAA due to the advantages of low-cost, simple operation and fast response.

3.6 Repeatability, stability, selectivity and reproducibility

The repeatability of the Cu(II)-PLH-CMWCNTs/PtE was investigated in 0.7 mM

SAA solution for 15 times with the same electrode (as shown in Fig. S7). The electrode showed a satisfying repeatability with a relative standard deviation (RSD) of 3.8%. The long-term stability of the prepared sensor was evaluated by examining the DPV current response toward 0.7 mM SAA every 15 days, and the dry electrodes were stored at room temperature before use. After three months, the response currents remained 94.7% (as shown in Fig. S8). The influences of some common structural analogues and electrochemically active substances in medicinal plants on the detection of SAA were also studied and the results were shown in Fig. 4. It was found that those interferents of 3,4-dihydroxy benzaldehyde (protocatechuic aldehyde, PA), 1,2-benzenediol (catechol, CC), glucose (Glu), ascorbic acid (AA) and uric acid (UA) did not affect the detection of SAA (signal variation < 3%). The reproducibility of the Cu(II)-PLH-CMWCNTs/PtE for the detection of SAA was evaluated using four modified electrodes prepared by the same method and the electrodes were determined under identified conditions(as shown in Fig. S9). With average RSD mean equal to 2.049% obtained, we have found the fabricated biosensor showed a better reproducibility.

3.7 Determination of SAA in real samples

To evaluate the practical applicability of the proposed biosensor, it was employed for the determination of SAA in real samples of extractives from *Salvia miltiorrhiza* and medicinal liquids (purchased from the local pharmacy). With proper amount of

the sample solution, the concentration of SAA could be calculated from the linear-regression equation of the standard solution, and the recovery was in a satisfactory rang of 98.64 ~ 103.88% (as shown in Table 1). The SAA concentrations in the real samples were compared statistically by the Student's *t*-test for accuracy with the results obtained by the HPLC method at the 95% confidence level. The *t*-test value was less than the critical value, indicated that there was no significant difference between the proposed and HPLC methods. Comparing with the HPLC method, the proposed method has the advantages of low-cost, simple, rapid and high-efficiency, it could be recommended for the SAA determination in real samples.

4. Conclusions

In this study, Cu(II)-PLH functionalized CMWCNTs were successfully synthesized and exploited as a novel mimetic enzyme for ultrasensitive electrochemical determination of SAA. Due to the excellent synergetic catalytic effect of copper redox-active units, and the aromatic π–π stacking interaction between PLH and CMWCNT, the obtained biosensor exhibited a high sensitivity of 0.27 μA μM^{-1} cm^{-2}, a wide linear range from 0.4 μM to 1000 μM and a low detection limit of 0.037 μM. With the good repeatability, stability and selectivity, the proposed sensor could be feasibly applied to detect SAA in real samples. In summary, this study provides a promising enzyme-mimicking material with potential applications in drug testing, biosensing, electroanalysis and relevant fields.

Acknowledgments

The financial supports from the National Natural Science Foundation of China (Grant nos. 81671779 and 81273993) are acknowledged.

Chen‐Long, B., Guang‐Rong, Z., 2015. Separation of salvianic acid A from the fermentation broth of engineered Escherichia coli using macroporous resins. J. Sep. Sci. 38(16), 2833-2840.

Fang, Y., Zhang, D., Guo, Y., Guo, Y., Chen, Q., 2015. Simple one-pot preparation of chitosan-reduced graphene oxide-Au nanoparticles hybrids for glucose sensing. Sens. Actuators B Chem. 221, 265-272.

J., M., S., A., C., T.P., M., V., A., R.S., P., S., 2007. Growth and characterization of L-histidine hydrochloride monohydrate single crystals. Cryst. Res. Technol. 42(1), 59-64.

Jiang, G., Gu, X., Jiang, G., Chen, T., Zhan, W., Tian, S., 2015. Application of a mercapto-terminated binuclear Cu(II) complex modified Au electrode to improve the sensitivity and selectivity for dopamine detection. Sens. Actuators B Chem. 209(Supplement C), 122-130.

Jun-ichi, U., Akira, H., 1984. Copper(II)–Poly(L-histidine) as an Enzyme Model for L-Ascorbate Oxidase. Bull. Chem. Soc. Jpn. 57(12), 3511-3516.

Levitzki, A., Pecht, I., Anbar, M., 1965. Oxidase-like Activity of the Copper (II) Poly-L-histidine Complex. Nat. 207(5004), 1386-1387.

Liu, R., Yu, X., Gao, W., Ji, D., Yang, F., Li, X., Chen, J., Tao, H., Huang, H., Yi, P., 2011.

Study on the interaction between salvianic acid A sodium and bovine serum albumin by spectroscopic methods. Spectrochimica Acta Part A: Molecular and Biomolecular Spectroscopy 78(5), 1535-1539.

Liu, X., Zhang, L., Wei, S., Chen, S., Ou, X., Lu, Q., 2014. Overoxidized polyimidazole/graphene oxide copolymer modified electrode for the simultaneous determination of ascorbic acid, dopamine, uric acid, guanine and adenine. Biosens. Bioelectron. 57(Supplement C), 232-238.

Lixia, P., Yuanwu, B., Haidi, W., Fan, Y., Bei, X., Shoubao, W., Xiuying, Y., Guanhua, D., 2008. A sensitive method for determination of salvianolic acid A in rat plasma using liquid chromatography/tandem mass spectrometry. Biomedical Chromatography 22(7), 786-794.

Ma, M., Miao, Z., Zhang, D., Du, X., Zhang, Y., Zhang, C., Lin, J., Chen, Q., 2015. Highly-ordered perpendicularly immobilized FWCNTs on the thionine monolayer-modified electrode for hydrogen peroxide and glucose sensors. Biosens. Bioelectron. 64, 477-484.

Pecht, I., Levitzki, A., Anbar, M., 1967a. The copper-poly-L-histidine complex. I. The environmental effect of the polyelectrolyte on the oxidase activity of copper ions. J. Am. Chem. Soc. 89(7), 1587.

Pecht, I., Levitzki, A., Anbar, M., 1967b. The copper-poly-L-histidine complex. I. The environmental effect of the polyelectrolyte on the oxidase activity of copper ions. J. Am. Chem. Soc. 89(7), 1587-1591.

Ramanathan, M., Patil, M., Epur, R., Yun, Y., Shanov, V., Schulz, M., Heineman, W.R., Datta, M.K., Kumta, P.N., 2016. Gold-coated carbon nanotube electrode arrays: Immunosensors for impedimetric detection of bone biomarkers. Biosens. Bioelectron. 77,

580-588.

Saleh, T.A., Gupta, V.K., 2011. Functionalization of tungsten oxide into MWCNT and its application for sunlight-induced degradation of rhodamine B. J. Colloid Interface Sci. 362(2), 337-344.

Vilian, A.T.E., Chen, S., 2014. Simple approach for the immobilization of horseradish peroxidase on poly-L-histidine modified reduced graphene oxide for amperometric determination of dopamine and H2O2. RSC Adv. 4(99), 55867-55876.

Wang, C.-Y., Ma, F.-L., Liu, J.-T., Tian, J.-W., Fu, F.-H., 2007. Protective Effect of Salvianic Acid A on Acute Liver Injury Induced by Carbon Tetrachloride in Rats. Biological and Pharmaceutical Bull. 30(1), 44-47.

Wang, X.-J., Wang, Z.-B., Xu, J.-X., 2005. Effect of salvianic acid A on lipid peroxidation and membrane permeability in mitochondria. J. Ethnopharmacology 97(3), 441-445.

Wang, X.-J., Xu, J.-X., 2005. Salvianic acid A protects human neuroblastoma SH-SY5Y cells against MPP+-induced cytotoxicity. Neurosci. Res. 51(2), 129-138.

Wang, X., You, Z., Sha, H., Cheng, Y., Zhu, H., Sun, W., 2014. Sensitive electrochemical detection of dopamine with a DNA/graphene bi-layer modified carbon ionic liquid electrode. Talanta 128, 373-378.

Weckhuysen Bert, M., Verberckmoes An, A., Vannijvel Ina, P., Pelgrims Josephina, A., Buskens Philip, L., Jacobs Pierre, A., Schoonheydt Robert, A., 1996. Zeolite Encaged Cu(Histidine) Complexes as Mimics of Natural Cu Enzymes. Angewandte Chem. International Edition in Engl. 34(23-24), 2652-2654.

Yan, X., Gu, Y., Li, C., Tang, L., Zheng, B., Li, Y., Zhang, Z., Yang, M., 2016. Synergetic

catalysis based on the proline tailed metalloporphyrin with graphene sheet as efficient mimetic enzyme for ultrasensitive electrochemical detection of dopamine. Biosens. Bioelectron. 77, 1032-1038.

Youyou, T., 2016. Artemisinin—A Gift from Traditional Chinese Medicine to the World (Nobel Lecture). Angewandte Chem. International Edition 55(35), 10210-10226.

Zhao, B.L., Jiang, W., Zhao, Y., Hou, J.W., Xin, W.J., 1996. Scavenging effects of salvia miltiorrhiza on free radicals and its protection for myocardial mitochondrial membranes from ischemia-reperfusion injury. Biochem. Mol. Biol. Int. 38(6), 1171-1182.

Zhao, D., Liu, H., Wang, F., Feng, Q., Li, M., 2013. A Simple, but Highly Sensitive, Graphene-based Voltammetric Sensor for Salvianic Acid A Sodium. Analytical Sci. 29(6), 625-630.

Zhao, T., Li, Y., Jiang, Q., Xu, Y., Jian, L., 2010. Simultaneous determination of sodium salvianic A baicalin,baicalein,wogonin,wogonoside and tanshinone A in chidan pills by HPLC, 1579-1581.

Zhi-ming, W., Tao, W., Yu-fen, T., Yan, L., Feng, R., Hao, W., 2007. Effects of Salvianolic Acid A on Oxidative Stress and Liver Injury Induced by Carbon Tetrachloride in Rats. Basic & Clinical Pharmacology & Toxicology 100(2), 115-120.

Figure captions

Fig. 1. TEM images of MWCNTs (A), CMWCNTs (B), PLH-CMWCNTs (C), and (D) EDX spectrum of Cu(II)-PLH-CMWCNTs. XPS spectra of the (E)

Cu(II)-PLH-CMWCNTs, (F) C1s, (G) N1s and (H) Cu2p. Inset shows the percentage of the components in the Cu(II)-PLH-CMWCNTs.

Fig. 2. Cyclic voltammograms of (A) bare PtE (curve a), CMWCNTs/PtE (b), PLH-CMWCNTs/PtE (c) and Cu(II)-PLH-CMWCNTs/PtE (d) recorded in 10 mM $K_3[Fe(CN)_6]$ solution with 0.1 M KCl; (B) bare PtE (a), CMWCNTs/PtE (b), PLH-CMWCNTs/PtE (c) and Cu(II)-PLH-CMWCNTs/PtE (d) toward 0.5 mM SAA; (C) Cu(II)-PLH-CMWCNTs/PtE toward 0, 0.3, 0.5 and 1.0 mM SAA. Scan rate: 50 mV s^{-1}.

Scheme 1. Proposed mechanism for the electrocatalytic oxidation of SAA at Cu(II)- PLH-CMWCNTs/PtE.

Fig. 3. (A) Differential pulse voltammograms (DPV) of SAA at the Cu(II)-PLH-CMWCNTs/PtE in PBS (pH 3.0) with different concentrations over the range of 0.1 μM to 3500 μM. (B) Calibration curve of the response currents vs. various SAA concentrations. Inset shows the low concentrations from 0.4 μM to 3.0 μM. Error bars=±standard deviation and n=5.

Fig. 4. Interference test of the Cu(II)-PLH-CMWCNTs/PtE in the presence of SAA upon the addition of different interferents including (A) 0.4 mM PA, 0.4 mM CC and 1 mM Glu; (B) 0.2 mM AA and 0.5 mM UA.

Table 1. Determination of SAA in real samples by the proposed biosensor.

Samp le	HPLC found/μ	RS D/%	This method	R SD/	Standa rd	Total found/μ	Recov ery/%

	M (n=5)		found/μM (n=5)	%	added/μM	M (n=5)	
Extractive 1[a]	49.77	1.37	50.43	2.01	50	102.37	103.88
Extractive 2[a]	57.36	2.04	59.09	1.86	100	157.93	98.84
Extractive 3[a]	64.08	1.51	63.87	2.35	150	214.62	100.05
Medicinal liquid 1[b]	604.60	2.14	610.12	2.06	50	659.87	99.50
Medicinal liquid 2[b]	534.34	1.67	531.49	1.79	100	630.13	98.64
Medicinal liquid 3[b]	510.05	2.09	514.36	2.18	150	667.42	102.04

[a] Extracted by soxhlet extractor method. [b] Diluted for 10 times.

Supporting captions

Scheme S1. Illustration in the preparation of Cu(II)-PLH-CMWCNTs/PtE.

Fig. S1. FTIR spectra of MWCNTs, CMWCNTs, PLH-CMWCNTs, and Cu(II)-PLH-CMWCNTs.

Fig. S2. Raman spectra of MWCNTs, CMWCNTs, PLH-CMWCNTs, and Cu(II)- PLH-CMWCNTs.

Fig . S3. XPS spectrum of the (a) CMWCNTs and (b) PLH-CMWCNTs.

Fig. S4. CVs of the (A) bare PtE; (B) CMWCNTs/PtE; (C)PLH-CMWCNTs/PtE; (D) Cu(II)-PLH-CMWCNTs/PtE in 0.1 M PBS (pH 3.0) in the absence (a) and presence (b) of 0.6 mM SAA.

Fig. S5. (A) Cyclic voltammograms of 0.5 mM SAA at the Cu(II)-PLH-CMWCNTs/PtE in PBS with different pH values (3.0~8.0). (B) The relationship between the formal peak potential (E0') and pH. Inset: the dependence of the anodic peak current on pH.

Fig. S6. (A) Cyclic voltammograms of 0.5 mM SAA at the Cu(II)-PLH-CMWCNTs/PtE in PBS with different scan rate (10, 20, 30, 40, 50, 60, 70, 80, 90, 100 mV s^{-1}). (B) Linear relationship of the redox peak currents (Ip) versus $v^{1/2}$.

Table S1. Determination of SAA with different mothod.

Fig. S7. Differential pulse voltammograms (DPV) of 0.7 mM SAA with the same Cu(II)-PLH-CMWCNTs/PtE for 15 times. Inset shows the peak points.

Fig. S8. Differential pulse voltammograms (DPV) current responses of 0.7 mM SAA with the same Cu(II)-PLH-CMWCNTs/PtE for a 15-day interval. Error bars=±standard deviation, n=5.

Fig. S9. CVs current responses of four different Cu(II)-PLH-CMWCNTs/PtE to 0.5 mM, 0.7 mM, 0.9 mM and 1.5 mM SAA in pH 7.0 PBS.

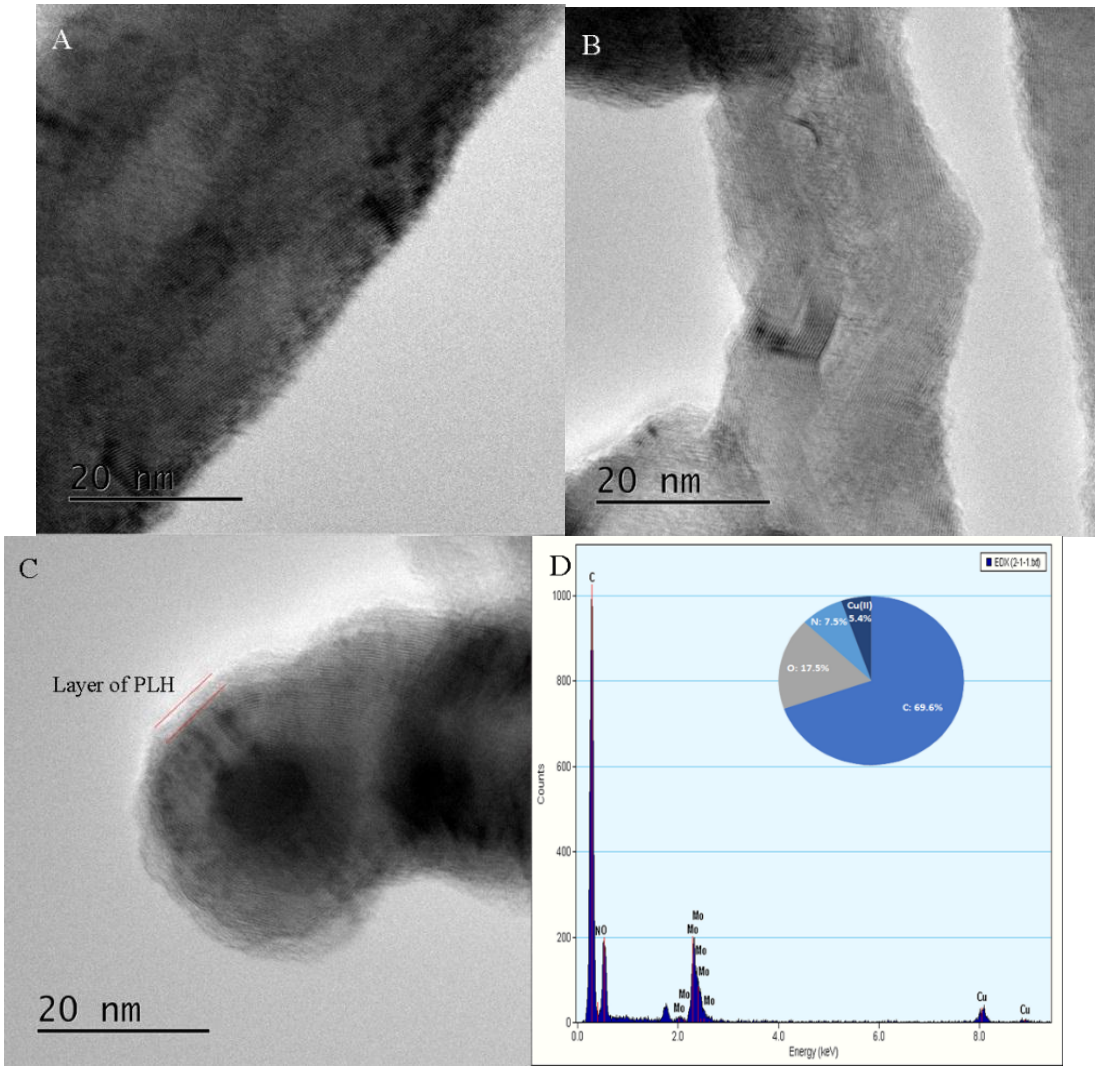

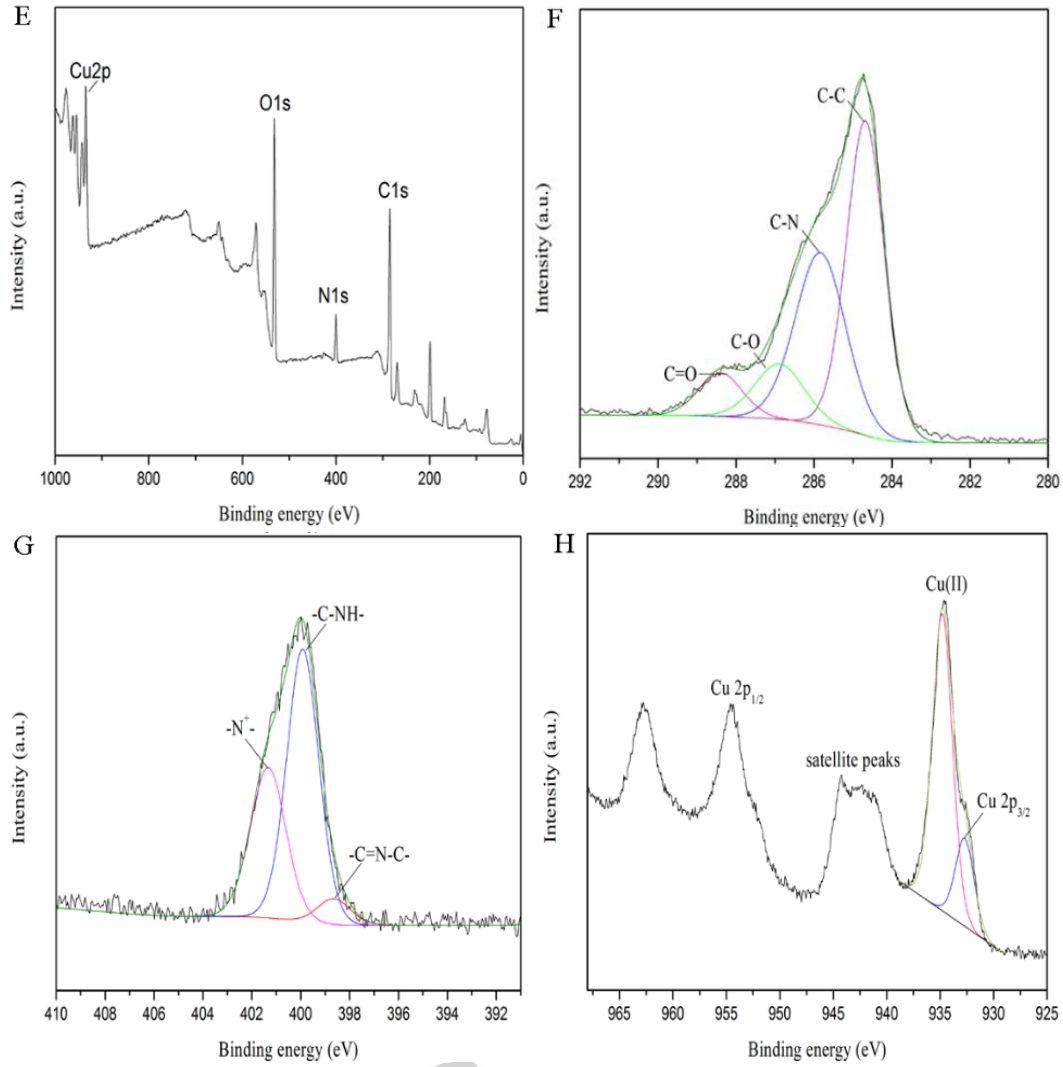
E
Cu2p
O1s
C1s
N1s
Intensity (a.u.)
1000
800
600
400
200
0
Binding energy (eV)
F
C-C
C-N
C-O
C=O
Intensity (a.u.)
292
290
288
286
284
282
280
Binding energy (eV)
G
-C-NH-
-N+-
-C=N-C-
Intensity (a.u.)
410
408
406
404
402
400
398
396
394
392
Binding energy (eV)
H
Cu(II)
Cu 2p1/2
satellite peaks
Cu 2p3/2
Intensity (a.u.)
965
960
955
950
945
940
935
930
925
Binding energy (eV)

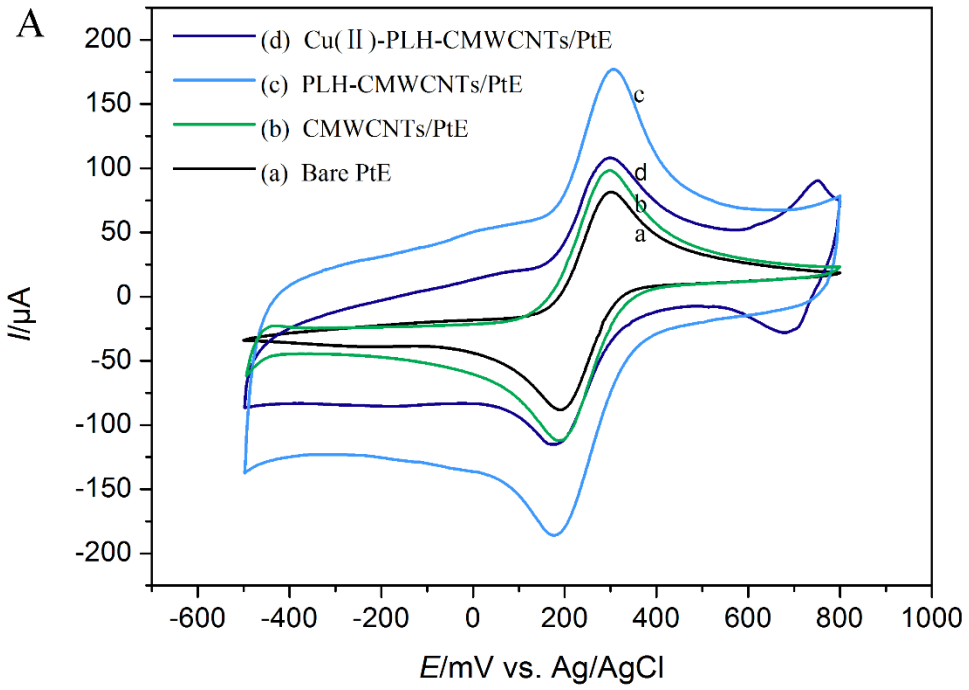
A
(d) Cu(Ⅱ)-PLH-CMWCNTs/PtE
(c) PLH-CMWCNTs/PtE
(b) CMWCNTs/PtE
(a) Bare PtE
c
d
b
a
I/μA
E/mV vs. Ag/AgCl

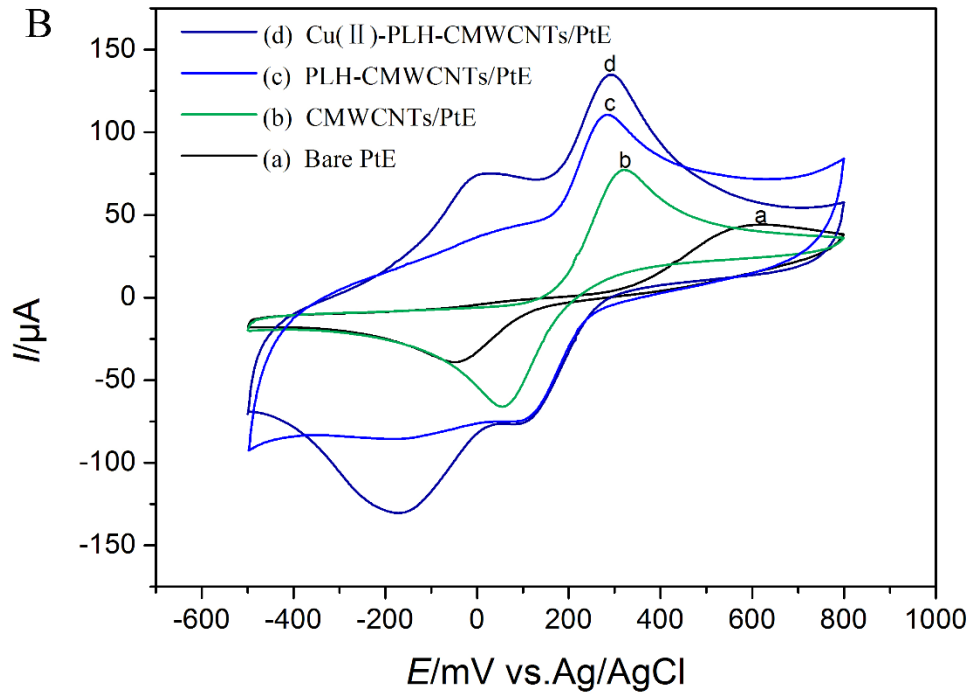
B
(d) Cu(Ⅱ)-PLH-CMWCNTs/PtE
(c) PLH-CMWCNTs/PtE
(b) CMWCNTs/PtE
(a) Bare PtE
d
c
b
a
I/μA
E/mV vs.Ag/AgCl

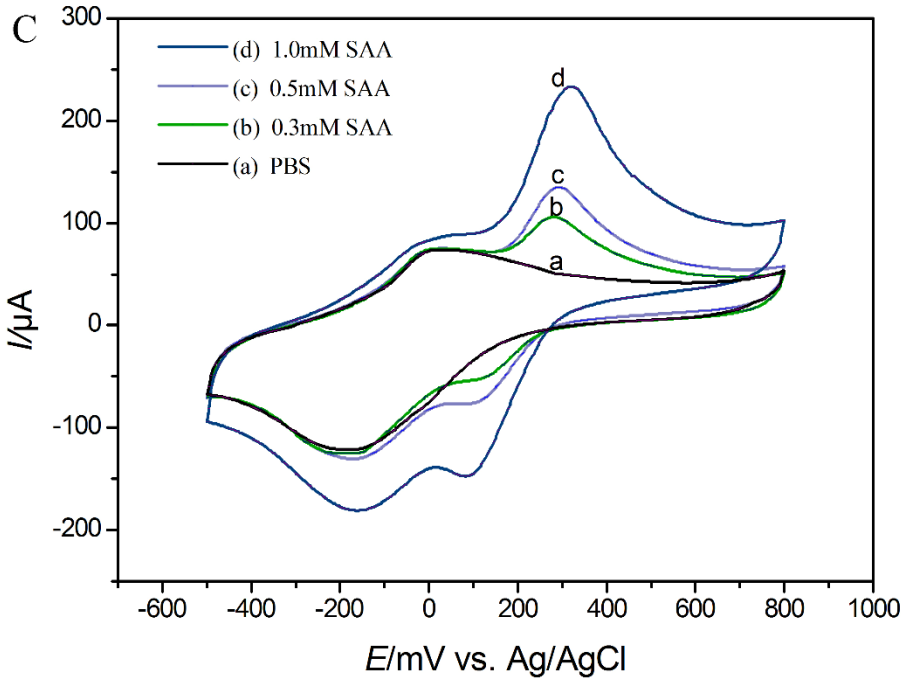

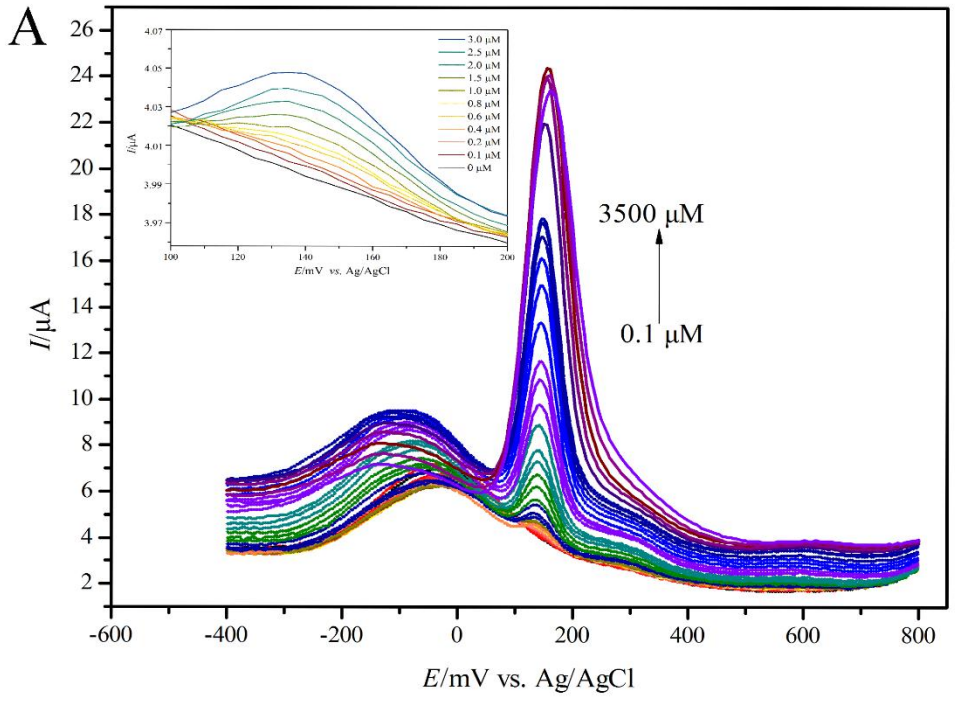
A
3500 μM
0.1 μM
I/μA
E/mV vs. Ag/AgCl
3.0 μM
2.5 μM
2.0 μM
1.5 μM
1.0 μM
0.8 μM
0.6 μM
0.4 μM
0.2 μM
0.1 μM
0 μM

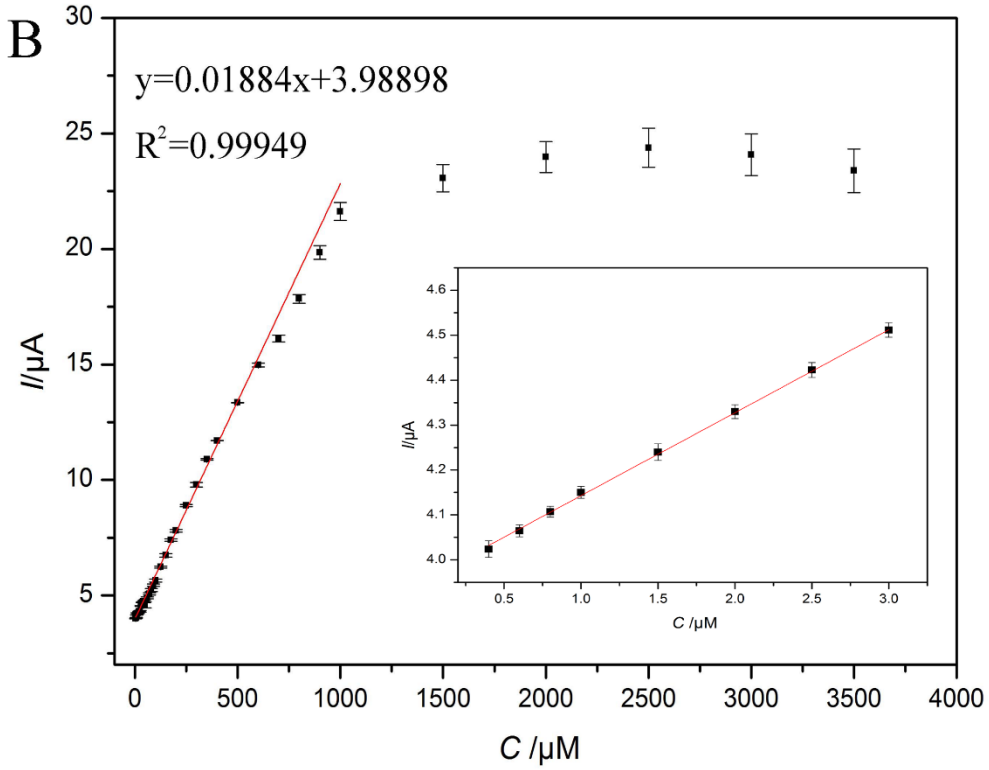
B
y=0.01884x+3.98898
R²=0.99949
I/μA
C /μM

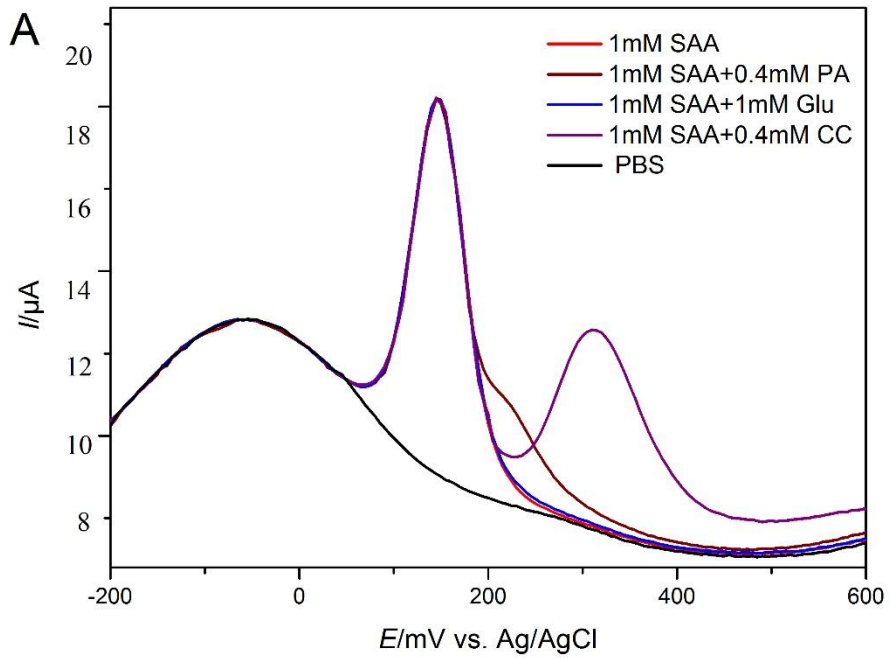
A
1mM SAA
1mM SAA+0.4mM PA
1mM SAA+1mM Glu
1mM SAA+0.4mM CC
PBS
I/μA
E/mV vs. Ag/AgCl

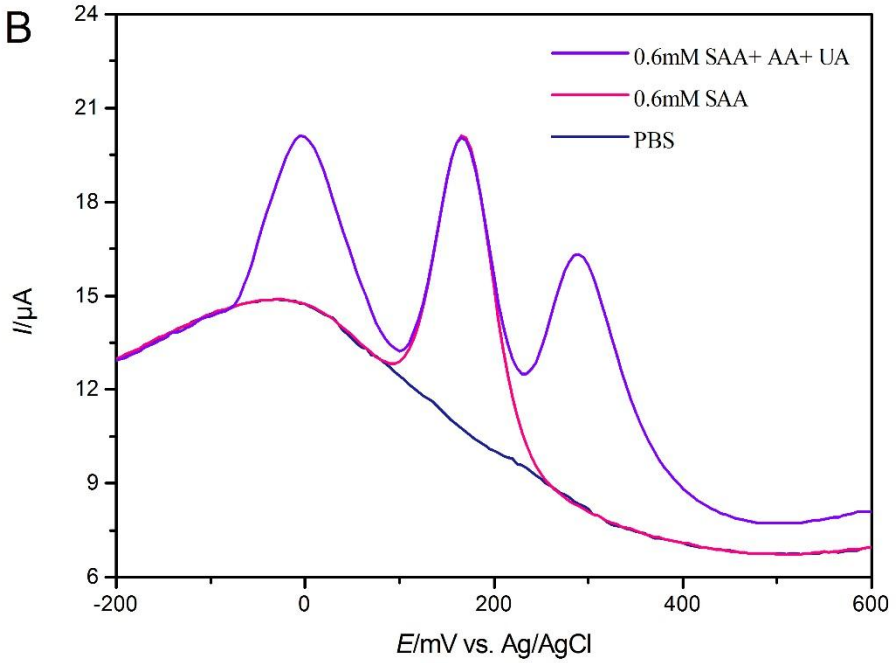
B
0.6mM SAA+ AA+ UA
0.6mM SAA
PBS
I/μA
E/mV vs. Ag/AgCl

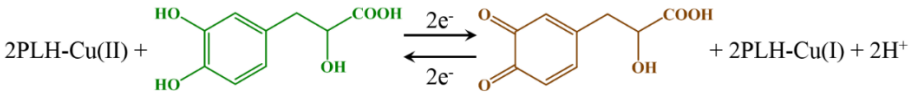

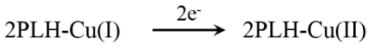

Highlights:

- Cu(II)-PLH-CMWCNTs nanocomposites was successfully synthesized and exhibited high catalytic performance
- Cu(II)-PLH-CMWCNTs was exploited as superior mimetic enzyme for the first time.
- The prepared biosensor exhibited catalytic ability to salvianic acid A.